



## Dielectric properties and relaxation dynamics in $\text{PbF}_2\text{-TeO}_2\text{-B}_2\text{O}_3\text{-Eu}_2\text{O}_3$ glasses

Akshatha WAGH, Y. RAVIPRAKASH, Sudha D. KAMATH

Department of Physics, Manipal Institute of Technology, Manipal University, Manipal 576104, India

Received 16 October 2014; accepted 25 January 2015

**Abstract:** Frequency and temperature dependent dielectric dispersion of  $20\text{PbF}_2\text{-}20\text{TeO}_2\text{-(}60\text{-}x\text{)B}_2\text{O}_3\text{-}x\text{Eu}_2\text{O}_3$  ( $x=0$  to 2.5, mole fraction, %) glasses prepared by the melt-quenching technique were investigated in the frequency range 1 Hz–10 MHz and temperature range 313–773 K. Dielectric relaxation dynamics was analyzed based on the electric modulus behavior. Dielectric losses ( $\tan \delta$ ) are found to be negligibly small in the temperature range 313–523 K, proving good thermal stability of the glasses. The present  $\text{Eu}_2\text{O}_3$ -doped oxyfluoroborate glasses showed low dielectric loss at higher frequency and lower temperature, proving their suitability for nonlinear optical materials.

**Key words:** doped glass; dielectric spectroscopy; electric modulus; AC conductivity; activation energy; Arrhenius equation

### 1 Introduction

The competition of speed, cost and reliability of opto-electronic devices in various applications has led to the research for new materials which can meet the distinct requirement. The rare earth(RE)-doped borate glasses are among those materials which have a number of optics and photonics applications. The contribution of these glasses in the last decade is highly promising that the research over various REs and their suitable host material has been studied. From this point of view, borate-based glasses are the best choice, which more clearly shows the relationship between glass structure and optical properties of RE ions. An interesting characteristic of the borate glass is the appearance of variations in its structural properties when RE cations are introduced [1–3]. The structure of the borate glasses is not a random distribution of  $\text{BO}_3$  triangles and  $\text{BO}_4$  tetrahedra, but a gathering of these units to form well-defined and stable borate groups such as diborate, triborate, tetraborate, that constitute the random three-dimensional network [1]. These units make the borate glasses as one of the best choices for RE doping. Borate glass is a suitable optical material for RE ions with high transparency, low melting point, high thermal stability, good RE ion solubility [2] and shows more

clear relationship between glass structure and physical properties. The addition of fluoride content to borate glasses decreases the phonon energy and increases the moisture resistance and transparency in the visible region, which in turn contribute to the reduction in the non-radiative losses. A large glass forming region also exists in the oxyfluoride systems with good and easy glass formation [3]. Lead fluoride gives some special significance with a good ability to form stable glasses over a wide range of concentrations due to dual role as glass modifier and glass former.  $\text{PbF}_2$  is a conditional glass former,  $\text{B}_2\text{O}_3$  is a glass forming oxide and with these two chemicals in the glass matrix, low rate of crystallization, moisture resistance, stable and transparent glasses have been achieved [3].

Among the possible REs, europium ( $\text{Eu}^{3+}$ ) is one of the most investigated and also one of the best optically active elements [1–3].  $\text{Eu}^{3+}$  is the most suitable rare earth element for investigating the inhomogeneities amongst the sites of the borate glass host because of its simpler electronic levels and glass network [4]. In particular, the addition of high field strength modifier, promoting the increase of the NBO species in the glass matrix, leads to the general depolymerisation of the network that can be related to the modifications of the optical and physical properties [3]. The trivalent  $\text{Eu}^{3+}$  ion is much favored among the RE elements because of its great importance

in various applications such as laser materials, sensors, high density frequency-domain optical memory, amplifiers for fiber optical communications active and inactive components in optical and photonic devices [5]. Due to technological importance of europium ion ( $\text{Eu}^{3+}$ ) and the advantages of above research,  $\text{Eu}_2\text{O}_3$ -doped lead fluoroborate glasses have been synthesized and investigated. A survey of literature shows that there are many reports available on quaternary borate glasses. The study of dielectric properties such as dielectric constant ( $\epsilon'$ ), loss tangent ( $\tan \delta$ ) and conductivity ( $\sigma(\omega)$ ) over a wide range of frequency and temperature of the glass materials not only helps in assessing the insulating characteristics and understanding the conduction phenomenon but also throws light on the structural aspects of the glasses to a large extent.

The purpose of the present work is to study the electrical conductivity and dielectric properties over a wide frequency range from 1 Hz to 10 MHz and a temperature range from 313 to 773 K for  $20\text{PbF}_2-20\text{TeO}_2-(60-x)\text{B}_2\text{O}_3-x\text{Eu}_2\text{O}_3$  glasses with various contents of  $\text{Eu}_2\text{O}_3$  (0.1%–2.5%).

## 2 Experimental

### 2.1 Sample preparation

A series of  $\text{Eu}^{3+}$ -doped lead fluoroborate glasses  $20\text{PbF}_2-20\text{TeO}_2-(60-x)\text{B}_2\text{O}_3-x\text{Eu}_2\text{O}_3$  (where  $x=0-2.5$ ) were prepared by the melt-quenching technique. The chemical powders were procured through Sigma Aldrich with purity <99%. These powders were thoroughly mixed in an agate mortar and pestle with respect to their glass compositions. The chemical compositions of the glasses with the name of samples are summarized in Table 1.

The thoroughly mixed chemical powders in the porcelain crucible were then kept for melting in an Indfurr electric furnace at 980 °C for 1.30 h. After the retirement of melting period, the molten mass is quenched rapidly on a stainless steel mould maintained at 200 °C. The glasses thus obtained were found to be

**Table 1** Chemical compositions of glasses

Glass code	$x(\text{Eu}_2\text{O}_3)/\%$	Glass composition
Eu <sub>0</sub>	0	$20\text{PbF}_2-20\text{TeO}_2-60\text{B}_2\text{O}_3$
Eu <sub>1</sub>	0.1	$20\text{PbF}_2-20\text{TeO}_2-59.9\text{B}_2\text{O}_3-0.1\text{Eu}_2\text{O}_3$
Eu <sub>2</sub>	0.5	$20\text{PbF}_2-20\text{TeO}_2-59.5\text{B}_2\text{O}_3-0.5\text{Eu}_2\text{O}_3$
Eu <sub>3</sub>	1.0	$20\text{PbF}_2-20\text{TeO}_2-59\text{B}_2\text{O}_3-1.0\text{Eu}_2\text{O}_3$
Eu <sub>4</sub>	1.5	$20\text{PbF}_2-20\text{TeO}_2-58.5\text{B}_2\text{O}_3-1.5\text{Eu}_2\text{O}_3$
Eu <sub>5</sub>	2.0	$20\text{PbF}_2-20\text{TeO}_2-58\text{B}_2\text{O}_3-2\text{Eu}_2\text{O}_3$
Eu <sub>6</sub>	2.5	$20\text{PbF}_2-20\text{TeO}_2-57.5\text{B}_2\text{O}_3-2.5\text{Eu}_2\text{O}_3$

clear, bubble free, transparent and yellowish in color. These samples were annealed at 200 °C for 3 h to remove induced residual thermal or mechanical stresses caused due to rapid quenching. Samples were then polished with different grain size emery polishing sheets. A thin coating of silver paint was applied on both sides of the sample to serve the purpose of dielectric measurement. The physical parameters like density, refractive of these glasses are given in Table 2.

**Table 2** Density, molecular mass and refractive of  $\text{PbF}_2-\text{TeO}_2-\text{B}_2\text{O}_3-\text{Eu}_2\text{O}_3$  glasses

Glass code	Molecular mass/( $\text{g}\cdot\text{mol}^{-1}$ )	Density, $\rho/(\text{g}\cdot\text{cm}^{-3})$	Refractive index $n$
Eu <sub>0</sub>	122.7309	3.8561	1.6254
Eu <sub>1</sub>	123.0132	3.8638	1.6875
Eu <sub>2</sub>	124.1424	3.8921	1.7112
Eu <sub>3</sub>	125.5539	3.9289	1.7460
Eu <sub>4</sub>	126.9655	3.9689	1.7511
Eu <sub>5</sub>	128.3770	4.0122	1.7567
Eu <sub>6</sub>	129.7886	4.0410	1.7690

### 2.2 X-ray diffraction

Powder X-ray diffraction (XRD) patterns for all the glass samples in the present investigation were recorded at room temperature using a Rigaku Miniflex 600 X-ray diffractometer with  $\text{Cu K}_\alpha$  radiation (40 kV and 15 mA) and a graphite monochromator with  $2\theta$  from 10° to 90°. XRD patterns of all glass samples are shown in Fig. 1.

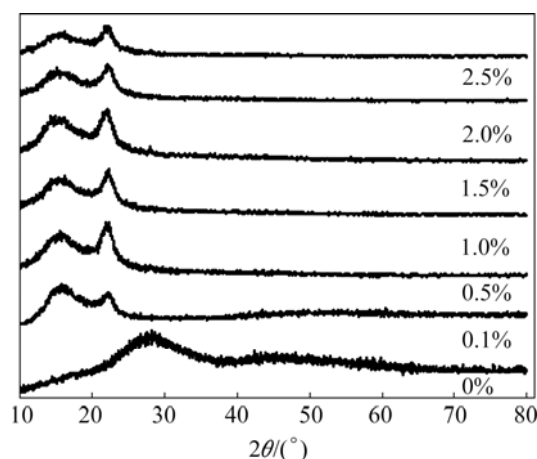


**Fig. 1** XRD patterns of powdered samples of  $\text{PbF}_2-\text{TeO}_2-\text{B}_2\text{O}_3-\text{Eu}_2\text{O}_3$  glass

### 2.3 Conductivity, impedance and dielectric measurement

The conductivity  $\sigma(\omega)$ , impedance ( $Z^*$ ), dielectric constant ( $\epsilon'$ ) and dielectric loss ( $\tan \delta$ ) measurements on the as-quenched (annealed) polished glass plates that

were silver painted were done using Novo Control Technologies Alpha Impedance Interface (S/N: ZG4-246/0) in the 1 Hz–10 MHz frequency range and temperature from 313 to 773 K. Based on these data, the dielectric constant was evaluated taking the dimensions and electrode geometry of the sample into account. All the dielectric data were collected while heating at a rate of 10 °C/min.

### 3 Results and discussion

The amorphous nature of the samples was ascertained by X-ray diffraction (XRD), as shown in Fig. 1. The XRD patterns of the samples show no discrete or continuous sharp peaks, confirming the amorphous nature of all the glass samples. A large broad peak around  $2\theta=25^\circ\text{--}30^\circ$  was observed, which is a typical feature of borate glass [6].

#### 3.1 Impedance analysis

To show the frequency dependent conductivity behavior of the present glasses at various temperatures, the real ( $Z'_p$ ) and the imaginary ( $Z''_s$ ) parts of the complex impedance ( $Z^* = Z'_p - jZ''_s$ ) are plotted against frequency, which are shown in Fig. 2 and Fig. 3, respectively. The frequency dependence of the real part ( $Z'_p$ ) of the complex impedance at different temperatures is shown in Fig. 2. From Fig. 2, it is clear that the impedance value is higher at lower temperatures in the low frequency region, and then it decreases gradually with the increase in both frequency and temperature. This decrease in  $Z'_p$  indicates a possible increase of the conductivity of the material. In the higher frequency domain ( $>0.4$  MHz), all curves merge, suggesting a possible release of space charge and a consequent lowering of the barrier properties in the

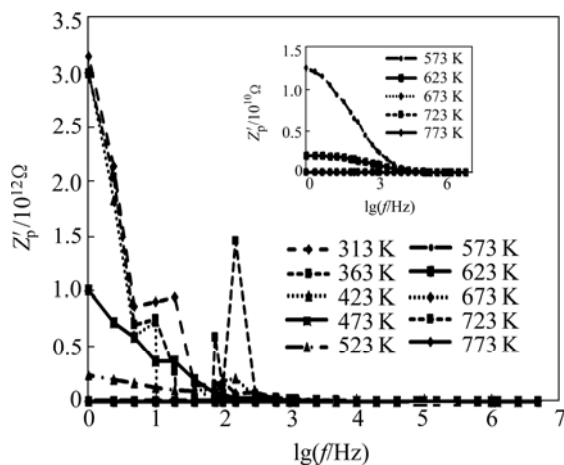


**Fig. 2** Frequency dependence of real part ( $Z'_p$ ) of impedance in temperature range 313–773 K of 2.5%  $\text{Eu}_2\text{O}_3$ -doped glass (Inset is the frequency dependence of real part ( $Z'_p$ ) of impedance range 573–773 K)

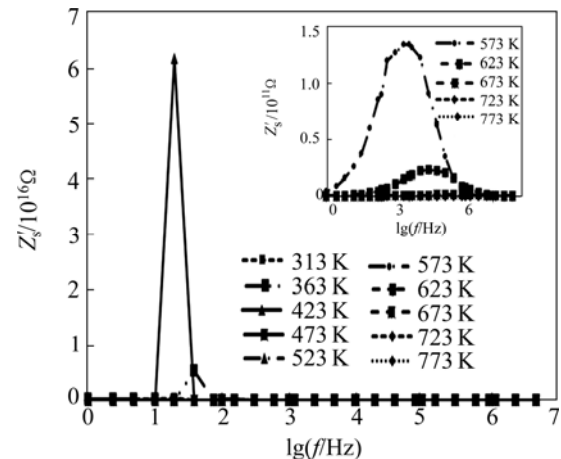


**Fig. 3** Frequency dependence of imaginary part ( $Z''_s$ ) of impedance in temperature range 313–773 K of 2.5%  $\text{Eu}_2\text{O}_3$ -doped glass (Inset is the frequency dependence of imaginary part ( $Z''_s$ ) of impedance range 623–773 K)

materials [7].

The variation of imaginary part of impedance ( $Z''_s$ ) with frequency at various temperatures is shown in Fig. 3. We can note that the imaginary part increases first with frequency for all temperatures reaching a maximum and then decreases as the frequency increases up to 70 kHz, and subsequently becomes frequency independent. Also,  $Z''_s$  at each temperature exhibits a relaxation peak whose peak frequency  $f_m$  shifts (as shown in the inset of Fig. 3) toward higher frequencies with the increase in temperature and follows the Arrhenius law. This tendency is apparently due to the presence of space charges in the material [7].

#### 3.2 Temperature dependence of AC electrical conductivity

Frequency dependence of total conductivity for 2.5%  $\text{Eu}_2\text{O}_3$ -doped glass at different temperatures is shown in Fig. 4.

The frequency dispersion characteristic in the frequency region has been analyzed using the Jonscher's universal power law relation [8]:

$$\sigma(\omega) = \sigma(0) + A\omega^s \quad (1)$$

where  $\sigma(0)$  is the frequency-independent DC conductivity of the glass sample.

The second term in the above relation gives AC conductivity ( $\sigma_{ac} = A\omega^s$ ), where  $A$  is temperature dependent constant and  $s$  is a material and temperature dependent power law exponent. At low frequencies ( $<5$  kHz), the conductivity is almost independent of frequency. Thus, the DC conductivity ( $\sigma(0)$ ) is a constant value. At low frequencies, random distribution of the ionic charge carriers via activated hopping gives rise to a frequency-independent conductivity while at higher

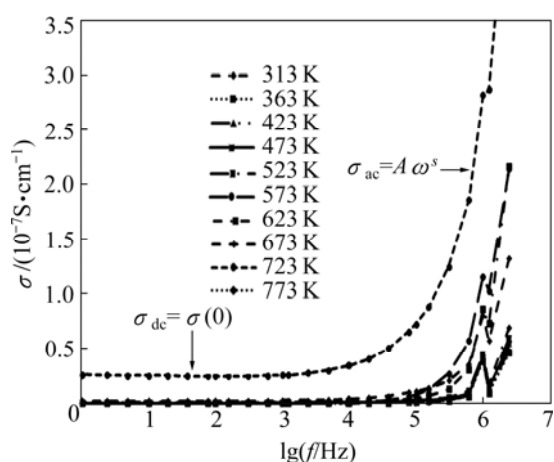


Fig. 4 Variation of AC conductivity ( $\sigma_{ac}$ ) with different frequencies at different temperatures

frequencies, conductivity exhibits dispersion which increases roughly in a power law fashion and eventually becomes almost linear at even higher frequencies [9].

Beyond 5 kHz, the conductivity increased apparently and became frequency independent. This may be due to the release of space charge at the electrode-sample interface. The change of the conductivity is shifted toward higher frequencies with the increase in temperature because mobile ions acquire more thermal energy and cross barrier more easily. At high frequency region, high dispersion has been observed. The high frequency dispersion is predominant at lower temperatures, and shifts to higher frequencies with increasing temperature which is clearly evident from Fig. 4. Temperature dependence of total conductivity ( $\sigma(\omega)$ ) at different frequencies 1, 10 and 100 kHz for 2.5%  $\text{Eu}_2\text{O}_3$ -doped glass is shown in Fig. 5. In the lower temperature region, 313–573 K, and the conductivity was temperature independent giving a constant DC conductivity ( $\sigma_{dc}$ ) value for all frequencies.

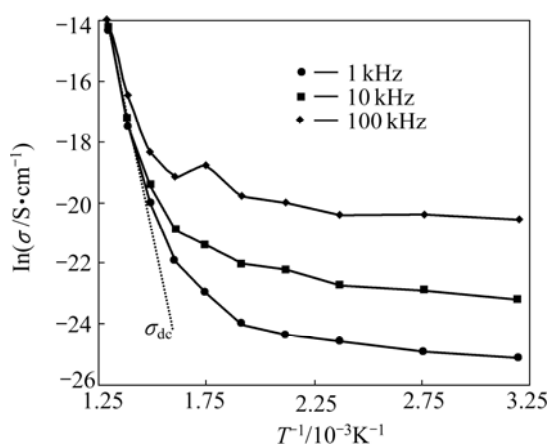


Fig. 5 Temperature dependence of conductivity ( $\sigma(\omega)$ ) at different frequencies 1, 10 and 100 kHz for 2.5%  $\text{Eu}_2\text{O}_3$  doped glass

In the temperature region of 573–773 K, conductivity increased rapidly giving AC component ( $\sigma_{ac}$ ) of the total conductivity  $\sigma(\omega)$ . It can be clearly observed that the conductivities at different frequencies appear to be approaching each other at higher temperatures. Also, the AC conductivity ( $\sigma_{ac}$ ) is observed to increase in both frequency and temperature and this can be attributed to the increase of the thermally activated small polarons hopping (SPH) [7]. The ionic conductivity in the present glass reaches a maximum value of  $6.86 \times 10^{-7}$  S/cm at 773 K.

### 3.3 Dielectric studies

The frequency dependence of the real ( $\epsilon'$ ) and imaginary ( $\epsilon''$ ) parts of dielectric constant and loss factor ( $\tan \delta$ ) are studied for the  $20\text{PbF}_2-20\text{TeO}_2-(60-x)\text{B}_2\text{O}_3-x\text{Eu}_2\text{O}_3$  ( $x=0.1-2.5$ ) glass samples in the temperature range 40–500 °C. Generally, the dielectric constant ( $\epsilon'$ ) of a material is determined by electronic, ionic, dipolar and space charge polarization [7–9]. The space charge distribution depends on the purity and the perfection of glass samples. Its influence is in general negligible at very low temperatures and noticeable in the low frequency region. The increase in dielectric constant of the sample with the increase in temperature is usually associated with the decrease in bond energies [10]. As the temperature increases, two effects on the dipolar polarization may occur: 1) it weakens the intermolecular forces and hence enhances the orientational vibration; 2) it increases the thermal agitation and hence strongly disturbs the orientational vibrations. The dielectric constant becomes larger at low frequencies and high temperatures and this can be taken as indication for spontaneous polarization [10]. This could be due to the fact that as the frequency increases, the polarizability contribution from ionic and orientation sources decreases and finally disappears due to their inertia.

Dielectric constant and loss factor are calculated using the following relations:

$$\epsilon' = -Z'_s / [\omega C_0 (Z_p'^2 + Z_s'^2)] \quad (2)$$

$$\epsilon'' = -Z'_p / [\omega C_0 (Z_p'^2 + Z_s'^2)] \quad (3)$$

where  $\omega=2\pi f$  is the angular frequency,  $C_0$  is the capacitance of the empty cell calculated from the geometry of the following relation:  $C_0 = \epsilon_0 B/t$ , where  $\epsilon_0$  is the permittivity of vacuum ( $8.854 \times 10^{-12}$  F/m),  $B$  and  $t$  are surface area and thickness of the glass sample, respectively. These measurements represent the distribution of ion energies or configurations in the structure and describe the electrical relaxation of the ionic glass as a microscopic property of the material [7]. The logarithmic frequency dependence of the real part ( $\epsilon'$ ) of the dielectric constant of 2.5% of  $\text{Eu}_2\text{O}_3$ -doped glass sample as a function of temperature is plotted in Fig. 6(a). From Fig. 6(a), it is evident that the dielectric

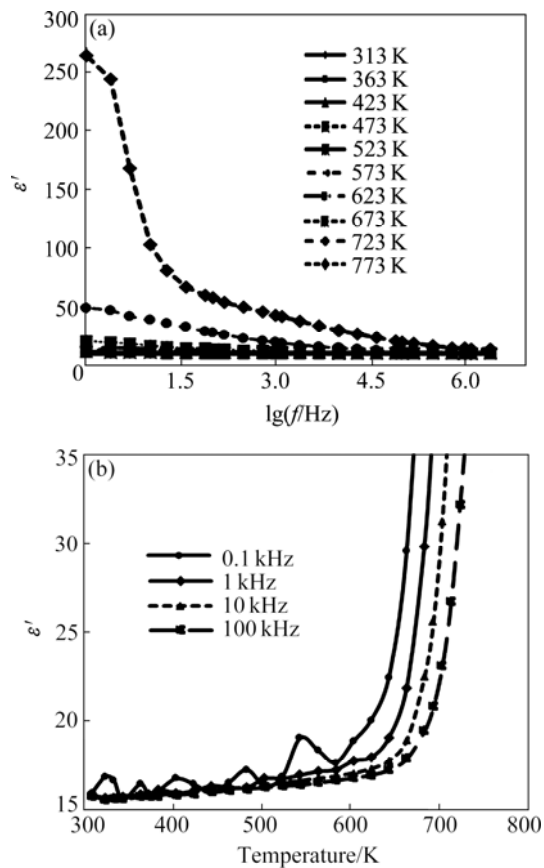


**Fig. 6** Variation of dielectric constant  $\epsilon'(\omega)$  with frequency of 2.5%  $\text{Eu}_2\text{O}_3$ -doped glass at different temperatures (a) and variation of dielectric constant with temperature of same glass at different frequencies (b)

constant  $\epsilon'$  increases with the increase in temperature at lower frequencies and reaches a low frequency plateau,  $\epsilon_p$  (value of the dielectric constant at quasistatic fields), usually associated with the polarization effects of the long range hopping of mobile ions with respect to the immobile glass matrix [11]. This increase in  $\epsilon'$ , in lower frequency and higher temperature region, may be due to the application of the field, which assists electron hopping between two different sites in the glasses. At high temperatures, the jump frequency of the charge carriers becomes large and comparable with the frequency of the applied field. Accordingly, at low frequency, the charge carriers hop easily out of the sites with high free energy barriers. This leads to a net polarization and gives an increase in the dielectric constant.

However, at higher frequency and lower temperature, the  $\epsilon'$  approaches a constant value, which results from rapid polarization processes that occur in the glass under applied field [11–18]. The charge carriers at higher frequency will no longer be able to rotate with enough speed, so their oscillation will begin to lag behind this field, resulting in a decrease in a dielectric

constant  $\epsilon'$ . At low temperatures, jump frequency of the charge carriers becomes smaller than the frequency of the applied field. The periodic reversal of the applied field takes place so rapidly that there are no excess charge carrier jumping in the field direction and the polarization due to charge piling up at high free energy barrier sites disappears, which lead to a decrease in the values of  $\epsilon'$  [12]. Also, the decrease in the dielectric constant with increasing frequency means that the response of the permanent dipoles decreases as the frequency increases [13–22]. At elevated temperature ( $>550$  K), the dielectric constant is rather high ( $>20$ ), and it falls against frequency at first and then becomes more or less stabilized down to above 153 Hz. The low value of dielectric constant at higher frequencies and lower temperatures is important for extending the material applications towards photonic and optoelectronic fields.

The temperature dependence of the dielectric constant  $\epsilon'$  at frequencies 0.1, 1, 10, 100 kHz, for 2.5%  $\text{Eu}_2\text{O}_3$ -doped glass sample is shown in Fig. 6(b). In the present work, dielectric properties of the glass samples were studied in the temperature range of 313–773 K. In the temperature range of 313–550 K, the sample of 2.5%  $\text{Eu}_2\text{O}_3$  glass has  $\epsilon'$  value in the range of 10–13 and above 550 K, it increases very rapidly above the glass transition at all frequencies under study. This behavior is typical to the polar dielectrics in which the orientation of dipoles is facilitated with rising temperature and thereby the dielectric constant is increased.

This is also due to the fact that, above the glass transition temperature, the viscosity of the glass continuously decreases and facilitates easy response of the ions to the external electric field which results in a rapid increase in the dielectric constant. Similar effect was observed for other samples also. This ensures thermal stability of these glasses up to 550 K and can be utilized for high temperature applications. From this plot, we can see the pronounced dielectric dispersion at lower frequency (0.1 kHz). Frequency dependence of the imaginary part of dielectric constant ( $\epsilon''$ ) for 2.5%  $\text{Eu}_2\text{O}_3$ -doped glass sample as a function of temperature is shown in Fig. 7(a). It is observed that  $\epsilon''$  also follows inverse dependence on frequency. At the lower frequencies and higher temperatures ( $>550$  K), the high values of  $\epsilon''$  are due to the migration of ions in the material. At the moderate frequencies,  $\epsilon''$  is due to the contribution of ion jump, conduction loss of ions migration and ion polarization loss [7]. At higher frequencies and lower temperatures, the ion vibrations may be the only source of dielectric loss which is minimal. Figure 7(b) shows minimal dielectric loss in the temperature range of 313–523 K. Figure 7(c) shows the variation of  $\epsilon''$  with temperature for various frequencies, 0.1, 1, 10, 100 kHz.

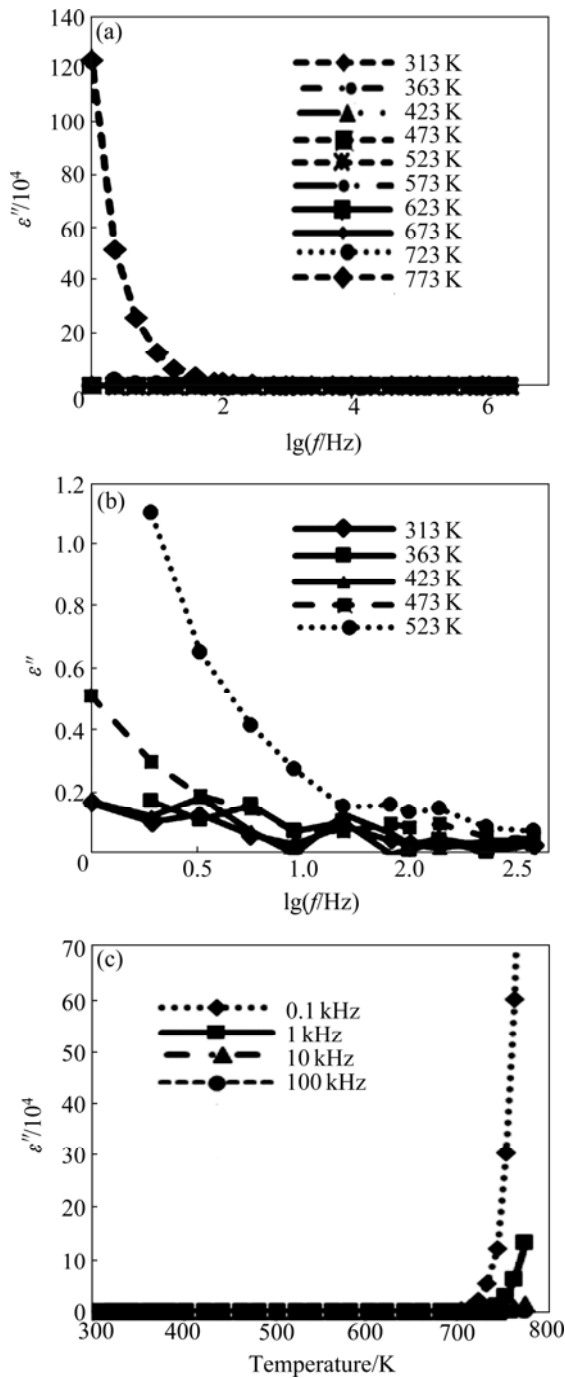


**Fig. 7** Variation of dielectric constant  $\varepsilon''(\omega)$  with frequency at different temperatures (313–773 K) of 2.5%  $\text{Eu}_2\text{O}_3$ -doped glass (a), variation of minimal dielectric loss with frequency at temperatures (313–523 K) (b), variation of dielectric constant  $\varepsilon''(\omega)$  with temperature at different frequencies (0.1–100 kHz) (c)

The factor which means the phase difference due to the loss of energy within the sample at different frequencies is the loss factor known as dielectric loss tangent, it is evaluated from the relation:

$$\tan \delta = \varepsilon''/\varepsilon' \quad (4)$$

This loss factor,  $\tan \delta$ , plays a very important role in

measuring the phase difference due to the loss of energy within a particular frequency. The frequency dependence of  $\tan \delta$  at different temperatures (313–773 K) for 2.5%  $\text{Eu}_2\text{O}_3$ -doped glass is shown in Fig. 8(a). At low frequencies (<150 Hz) and high temperatures (>550 K), the dielectric loss values are found to be high and then decrease with frequency and increase with temperature. Figure 8(b) shows variation of loss factor  $\tan \delta$  with

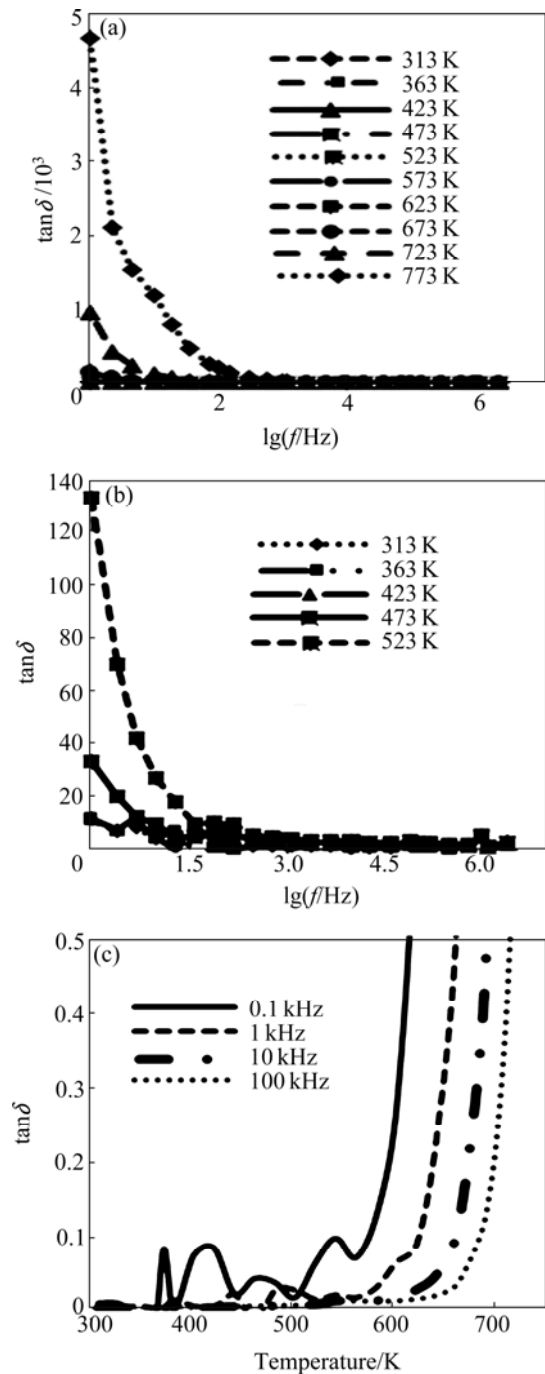


**Fig. 8** Variation of loss factor,  $\tan \delta$  with frequency at different temperatures (313–773 K) of 2.5%  $\text{Eu}_2\text{O}_3$ -doped glass sample (a), variation of loss factor  $\tan \delta$  with frequency at temperatures (313–523 K) (b), variation of loss factor  $\tan \delta$  with temperature at different frequencies (0.1–100 kHz) (c)

frequency at temperatures (313–523 K) and it is evident that the dielectric loss  $\tan \delta$ , below 550 K is in the range of 0.00086–0.2, negligibly small. This may be due to the rapid response of active component than its reactive component.

At higher frequencies, the loss tangent decreases with increasing frequency because the reactive component increases in proportion to the frequency whereas the active component of the current is practically independent of frequency [11]. Figure 8(c) shows the variation of loss factor,  $\tan \delta$  with temperature at different frequencies (0.1–100 kHz). This plot shows shifting of  $\tan \delta$  curve to higher frequency with increasing temperature.

The loss factor,  $\tan \delta$ , of the  $20\text{PbF}_2\text{-}20\text{TeO}_2\text{-(}60-x\text{)B}_2\text{O}_3\text{-}x\text{Eu}_2\text{O}_3$  ( $x=0.1$  and  $2.5$ ) as a function temperature at various frequencies 1 kHz and 10 kHz is shown in Fig. 9. It is found that the loss factor,  $\tan \delta$ , decreases with the partial replacement of  $\text{B}_2\text{O}_3$  by  $\text{Eu}_2\text{O}_3$  and decreases with increase in frequency and increases with increase in temperature.

The frequency dependence of quality factor,  $Q$ , for 2.5%  $\text{Eu}_2\text{O}_3$ -doped glass at different temperatures is shown in Fig. 10. It is clearly visible from Fig. 10 that,

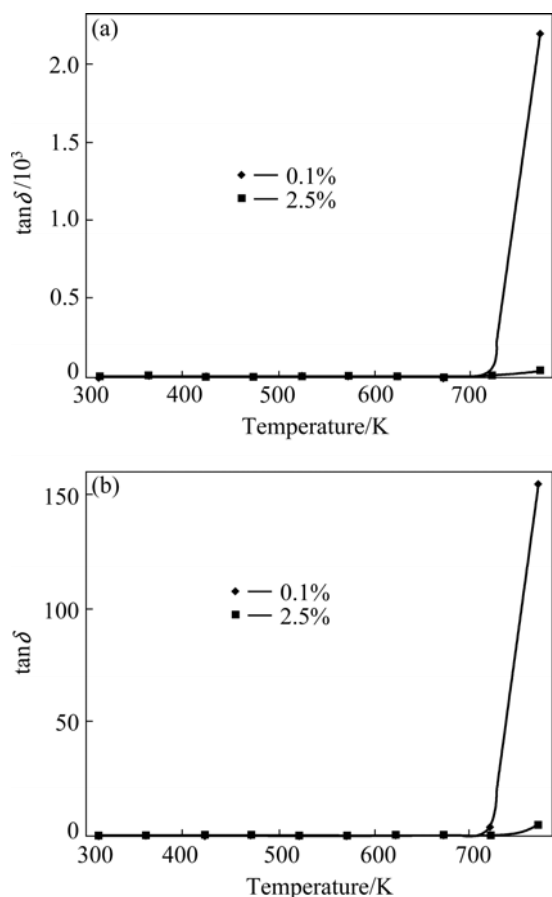


**Fig. 9** Loss factor,  $\tan \delta$ , of  $20\text{PbF}_2\text{-}20\text{TeO}_2\text{-(}60-x\text{)B}_2\text{O}_3\text{-}x\text{Eu}_2\text{O}_3$  ( $x=0.1\%$  and  $2.5\%$ ) as function of temperature at various frequencies: (a) 1.0 kHz; (b) 10 kHz

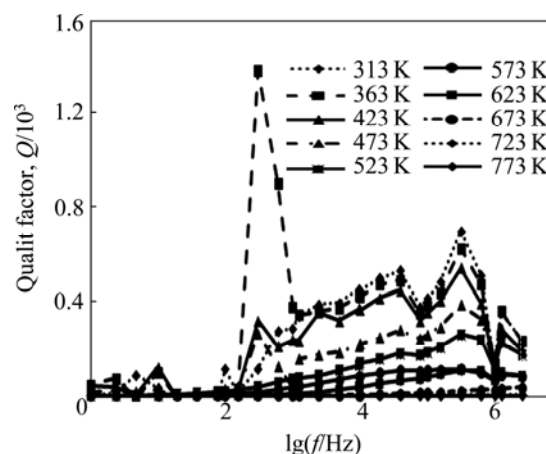


**Fig. 10** Variation of quality factor  $Q$  versus frequency for 2.5%  $\text{Eu}_2\text{O}_3$  doped glass at different temperatures

the dielectric loss decreases and the quality factor  $Q$  ( $=1/\tan \delta$ ) increases with increasing frequency. The low values of dielectric loss and high values of  $Q$  factor, at higher frequencies and lower temperatures indicate that the prepared  $\text{Eu}_2\text{O}_3$ -doped glasses are of good quality. The low dielectric loss at higher frequency and lower temperature is of fundamental use for nonlinear optical materials in their application [11–15].

### 3.4 Modulus studies

The study of electric modulus will justify electrical relaxation behavior in ion conducting material. Electric modulus formalism is useful to understanding the bulk responses of electrical properties of a material as electrode polarization effects are minimized.

The electric modulus is defined as

$$M' = \epsilon' / ((\epsilon')^2 + (\epsilon'')^2) \quad \text{and} \quad M'' = \epsilon'' / ((\epsilon')^2 + (\epsilon'')^2) \quad (5)$$

where  $M'$  and  $M''$  are real and imaginary parts of complex permittivity.

The frequency dependence of  $M'$  and  $M''$  at different temperatures for 2.5%  $\text{Eu}_2\text{O}_3$ -doped glass is shown in Fig. 11. Similar nature of frequency dependence is observed for other glass composition.

These figures clearly exhibit the relaxation characteristics of dielectric properties of these glasses. It should be noted from Fig. 11(a) that  $M'$  increases with increasing temperature and at sufficiently high temperature reaches a plateau which is constant value at high frequencies and it tends to zero at low frequencies, suggesting negligible or absent electrode polarization phenomenon [11]. The imaginary part of the electric modulus  $M''$  as a function at several temperatures is shown in Fig. 11(b). The shape of the spectrum remains the same but the  $M''_{\text{max}}$  peak frequency ( $f_{\text{max}}$ ) shifts towards higher frequencies side as the temperature increases. The shift in  $M''$  peak maximum corresponds to the conductivity relaxation.

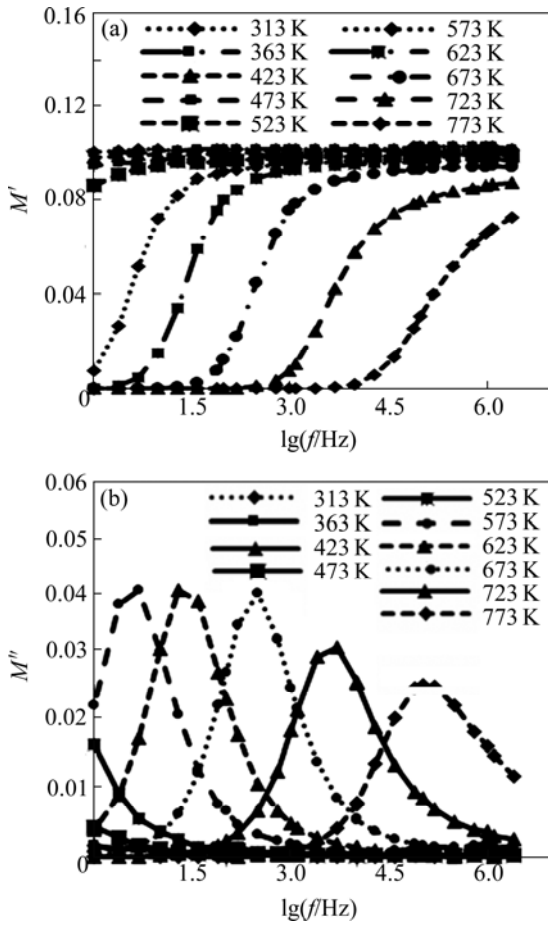


Fig. 11 Frequency dependence of  $M'$  (a) and  $M''$  (b) at different temperatures for 2.5%  $\text{Eu}_2\text{O}_3$ -doped glass

The maximum in the  $M''$  (Fig. 11(b)) peak shifts to higher frequency with increasing temperature. The frequency region below peak maximum  $M''$  ( $<f_{\text{max}}$ ) determines the range in which charge carriers are mobile on long distances. At a frequency above peak maximum  $M''$  ( $>f_{\text{max}}$ ), the carriers are spatially restricted to potential wells, being mobile on short distances makes only localized motion within wells. The way the imaginary part of complex modulus  $M''$  varies with frequency suggests the spread of relaxation time. Such spread is possibly due to the coupling of individual relaxation processes. One site needs to relax before others can do so. This behavior suggests that the dielectric relaxation is thermally activated where hopping mechanism of charge carriers dominate, intrinsically.

Relaxation time ( $\tau$ ) was calculated from  $\tau=1/2\pi f_{\text{max}}$  with condition  $\omega_c\tau_c=1$  (where  $\omega_c=1/2\pi f_{\text{max}}$ ) and plotted as  $\lg \tau$  vs  $1000/T$ . The variation of logarithmic relaxation time with temperature of 2.5%  $\text{Eu}_2\text{O}_3$ -doped glass sample is shown in Fig. 12. The plot is found to be linear and fitted using the Arrhenius relation:

$$\tau_r = \tau_0 \exp[-E_a/(k_B T)] \tag{6}$$

where  $\tau_0$  is the pre-exponential factor and  $E_a$  is the

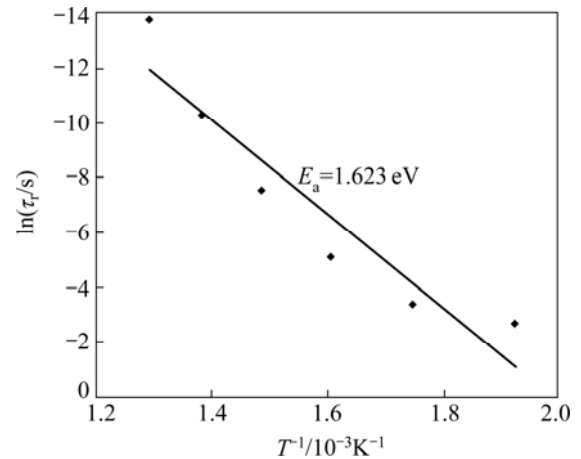


Fig. 12 Variation of relaxation time with temperature of 2.5%  $\text{Eu}_2\text{O}_3$  doped glass sample

activation energy for relaxation;  $k_B$  is the Boltzmann constant and  $T$  is the thermodynamic temperature. The activation energy ( $E_a$ ) calculated from the slope of the fitted line is found to be 1.623 eV for 2.5%  $\text{Eu}_2\text{O}_3$ -doped glass system. The partial replacement of  $\text{B}_2\text{O}_3$  with  $\text{Eu}_2\text{O}_3$  will create more NBOs. This factor, besides the weaker bond strength of  $\text{Eu}-\text{O}$  (473 kJ/mol) compared with that of  $\text{B}-\text{O}$  (809 kJ/mol), will affect the physical properties.

### 4 Conclusions

The frequency and temperature dependence of dielectric properties of  $\text{PbF}_2\text{-TeO}_2\text{-B}_2\text{O}_3$  of glasses doped with 0.1%–2.5%  $\text{Eu}_2\text{O}_3$  were investigated in the frequency range of 1 Hz–10 MHz and temperature range of 313–773 K. The dielectric dispersion was found to occur for the investigated amorphous samples in the audio frequency range. The magnitude of the frequency dispersion depends on the temperature and largely noticeable as temperature increases. The increase of  $\text{Eu}_2\text{O}_3$  content with replacement of  $\text{B}_2\text{O}_3$  varied the dielectric properties of the studied glass system  $\text{PbF}_2\text{-TeO}_2\text{-B}_2\text{O}_3\text{-Eu}_2\text{O}_3$ . The loss factor,  $\tan \delta$ , decreased with the partial replacement of  $\text{B}_2\text{O}_3$  by  $\text{Eu}_2\text{O}_3$  and decreased with increase in frequency and increased with increase in temperature. Dielectric losses decreased with increase in  $\text{Eu}_2\text{O}_3$  content. The activation energy of 2.5%  $\text{Eu}_2\text{O}_3$  was found to be 1.623 eV. The low values of dielectric loss and high values of  $Q$  factor, at higher frequencies and lower temperatures indicated that the prepared  $\text{Eu}_2\text{O}_3$  doped glasses are of good quality. The present  $\text{Eu}_2\text{O}_3$ -doped oxyfluoroborate glasses showed low dielectric loss at higher frequency and lower temperature, proving their suitability for nonlinear optical materials.



## Acknowledgments

This work was supported by a grant-in-aid for a scientific research from the Department of Atomic Energy (DAE)-Board of Research in Nuclear Science [S.No. 2012/34/17/BRNS] of the Government of India. Authors thank UGC-DAE Consortium for Scientific Research Centre for providing Dielectric measurement facility for characterizing the research samples.

## References

- [1] MARIMUTHU K, KARUNAKARAN R T, SURENDRA BABU S, MURALIDHARAN G, ARUMUGAM S, JAYASANKAR C K. Structural and spectroscopic investigations on  $\text{Eu}^{3+}$  doped alkali fluoroborate glasses [J]. *Solid State Sciences*, 2009, 11: 1297–1302.
- [2] SADDEEK Y B. Structural analysis of alkali borate glasses [J]. *Physica B: Condensed Matter*, 2004, 344: 163–175.
- [3] DEVA PRASAD RAJU B, MADHUKAR REDDY C. Structural and optical investigations of  $\text{Eu}^{3+}$  ions in lead containing alkali fluoroborate glasses [J]. *Optical Materials*, 2012, 34: 1251–1260.
- [4] MAHATO K K, RAI S B, RAI A. Optical studies of  $\text{Eu}^{3+}$  doped oxyfluoroborate glass [J]. *Spectrochimica Acta, Part A*, 2004, 60: 979–985.
- [5] KIRAN N.  $\text{Eu}^{3+}$  ion doped sodium–lead borophosphate glasses for red light emission [J]. *Journal of Molecular Structure*, 2014, 1065–1066: 93–98.
- [6] GAO G, HU L L, FAN H Y, WANG G N, LI K F, FENG S Y, FAN S J, CHEN H Y. Effect of  $\text{Bi}_2\text{O}_3$  on physical, optical and structural properties of boron silicon bismuthate glasses [J]. *Optical Materials*, 2009, 32: 159–163.
- [7] HRAIECH S, FERID M. Synthesis, electrical and dielectric properties of  $(\text{Na}_2\text{O})_{0.5}-(\text{P}_2\text{O}_5)_{0.5}$  glass [J]. *Journal of Alloys and Compounds*, 2013, 577: 543–549.
- [8] JONSCHER A K. The ‘universal’ dielectric response [J]. *Nature*, 1977, 267: 673–679.
- [9] SALMAN F. Dielectric characteristics of  $\text{CuO}-\text{Na}_2\text{O}-\text{SiO}_2$  glasses with Cole–Cole plots technique and AC conductivity study [J]. *Glass Physics and Chemistry*, 2013, 39: 150–154.
- [10] MAHMOUD K H, ABDEL-RAHIM F M, ATEF K, SADDEEK Y B. Dielectric dispersion in lithium–bismuth–borate glasses [J]. *Current Applied Physics*, 2011, 11: 55–60.
- [11] LANGAR A, SDIRI N, ELHOUCHEH H, FERID M. Conductivity and dielectric behavior of  $\text{NaPO}_3-\text{ZnO}-\text{V}_2\text{O}_5$  glasses [J]. *Journal of Alloys and Compounds*, 2014, 590: 380–387.
- [12] GEDAM R S, RAMTEKE D D. Electrical, dielectric and optical properties of  $\text{La}_2\text{O}_3$  doped lithium borate glasses [J]. *Journal of Physics and Chemistry of Solids*, 2013, 74: 1039–1044.
- [13] SHAPAAN M, EBRAHIM F M. Structural and electric–dielectric properties of  $\text{B}_2\text{O}_3-\text{Bi}_2\text{O}_3-\text{Fe}_2\text{O}_3$  oxide glasses [J]. *Physica B*, 2010, 405: 3217–3222.
- [14] SUJATHA T, KUMARA SATISH, SANKARAPPA T, DEVIDASA G B, HANAGODIMATH S M. Conductivity studies in some  $\text{CaO}$  and  $\text{ZnO}$  doped vanadophosphate glasses [J]. *International Journal of Engineering Research and Applications*, 2013, 3: 588–596.
- [15] SALEM SHAABAN M, MOHAMED E A. Electrical conductivity and dielectric properties of  $\text{Bi}_2\text{O}_3-\text{Ge}_2\text{O}_3-\text{PbO}-\text{MoO}_3$  glasses [J]. *Journal of Non-Crystalline Solids*, 2011, 357: 1153–1159.
- [16] NAGARAJA N, SANKARAPPA T, SUJATHA T. DC and dielectric relaxation studies in  $\text{CuO}$  doped borate glasses [J]. *International Journal of Engineering Science and Innovative Technology*, 2014, 3: 284–289.
- [17] WAGEH S, HIGAZY ANWER A, ALGRADEE MOHAMMED A. Optical properties and activation energy of a novel system of  $\text{CdTe}$  nanoparticles embedded in phosphate glass matrix [J]. *Journal of Modern Physics*, 2011, 2: 913–921.
- [18] DURGA D K, VEERAAIAH N. Dielectric dispersion in  $\text{ZnF}_2-\text{Bi}_2\text{O}_3-\text{TeO}_2$  glass system [J]. *Journal of Materials Science*, 2001, 365: 625–632.
- [19] EL-FALAKYAN GHADA E, GUIRGUISA OSIRIS W, ABDEL-AAL NADIA S A C. conductivity and relaxation dynamics in zinc-borate glasses [J]. *Progress in Natural Science: Materials International*, 2012, 22: 86–93.
- [20] SRINIVASA RAO L, SRINIVASA REDDY M, KRISHNA RAO D, VEERAAIAH N. Influence of redox behavior of copper ions on dielectric and spectroscopic properties of  $\text{Li}_2\text{O}-\text{MoO}_3-\text{B}_2\text{O}_3$ :  $\text{CuO}$  glass system [J]. *Solid State Sciences*, 2009, 11: 578–587.
- [21] SONG J, CHEN G H, YUAN C L, YANG Y. Effect of the  $\text{Sr}/\text{Ba}$  ratio on the microstructures and dielectric properties of  $\text{SrO}-\text{BaO}-\text{Nb}_2\text{O}_5-\text{B}_2\text{O}_3$  glass–ceramics [J]. *Materials Letters*, 2014, 117: 7–9.
- [22] LIU Tao-yong, CHEN Guo-hua, SONG Jun, YUAN Chang-lai. Crystallization kinetics and temperature dependence of energy storage properties of niobate glass-ceramics [J]. *Transactions of Nonferrous Metals Society of China*, 2014, 24(3): 729–735.

# $\text{PbF}_2-\text{TeO}_2-\text{B}_2\text{O}_3-\text{Eu}_2\text{O}_3$ 玻璃介电性能和弛豫动力学

Akshatha WAGH, Y. RAVIPRAKASH, Sudha D. KAMATH

Department of Physics, Manipal Institute of Technology, Manipal University, Manipal 576104, India

**摘要:** 在频率范围为 1 Hz~10 MHz 和温度范围为 313~773 K 条件下, 采用熔炼–淬火技术制备  $20\text{PbF}_2-20\text{TeO}_2-(60-x)\text{B}_2\text{O}_3-x\text{Eu}_2\text{O}_3(x=0\sim 2.5, \text{摩尔分数, \%})$  玻璃, 并研究频率和温度对介电性能的影响。通过介电模量行为分析材料的介电弛豫动力学。在 313~523 K 温度范围内, 介电损失可以忽略不计, 表明玻璃具有良好的热稳定性。所制备的  $\text{Eu}_2\text{O}_3$  掺杂氧氟硼玻璃在高频低温下介电损失低, 是非线性光学材料。

**关键词:** 掺杂玻璃; 介电光谱学; 介电模量; 交流电导率; 激活能; Arrhenius 方程

(Edited by Yun-bin HE)